Aerodynamic performance analysis of a trailing-edge flap for wind turbines

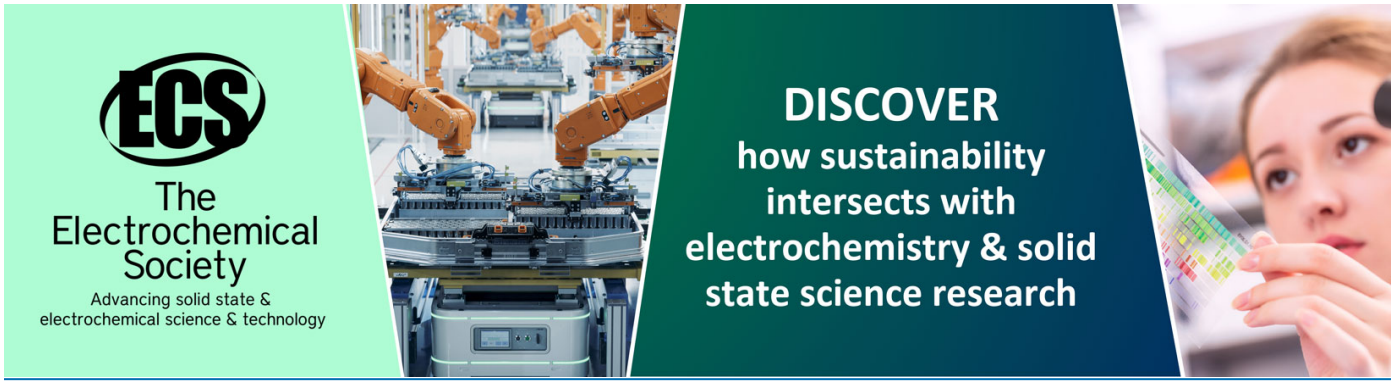

IOP Conf. Series: Journal of Physics: Conf. Series **1037** (2018) 022020 doi:10.1088/1742-6596/1037/2/022020

Aerodynamic performance analysis of a trailing-edge flap for wind turbines

Xu Bofeng*[1], Feng Junheng[1], Li Qing[2], Xu Chang[1], Zhao Zhenzhou[1], Yuan Yue[1]

[1] College of Energy and Electrical Engineering, Hohai University, Nanjing 211100, China

[2] China Electric Power Research Institute, Beijing 100192, China

E-mail: bfxu1985@hhu.edu.cn

Abstract: In this paper, a trailing-edge flap is designed based on the wind turbine airfoil S809. The aerodynamic performance and flowfield of the proposed trailing-edge flap airfoil are predicted by computational fluid dynamics (CFD) at angles of attack from -5° to 12.5°. The lift coefficient, drag coefficient, pressure contour, and streamline distribution of the proposed trailing-edge flap airfoil are analyzed and then compared with those of the traditional flaps. The results illustrate that the lift coefficient and the lift-to-drag ratio of the trailing-edge flap are markedly larger than those of the traditional flaps and that the trailing-edge flap can effectively improve the stall characteristics of the trailing-edge airfoil.

1. Introduction

With the depletion of global fossil energy and worsening of environmental problems, wind energy, as the most easily accessible clean energy, has drawn wide interest and has become an important direction for new energy development worldwide. The trend in large-scale wind turbines, aimed at lowering the cost per kWh, has been a primary target of research and development. However, the large-scale trend in wind turbines can inevitably lead to increasing in blade size and quality [1]. The following problems should be solved:

- The blades of large-scale wind turbines have high inertia, and single-variable pitch control can hardly cope with rapidly changing aerodynamic loads under turbulent wind conditions [2].
- The frequent use of the variable pitch control system can easily cause fatigue failure in the variable pitch device [3].
- The large-scale wind turbine has a high tower and a large impeller radius; thus, wind shear and tower shadow can exert large, negative effects on fan operation [1].

These above problems can be alleviated by using the blades of a wind turbine with a trailing-edge flap. The airfoil with a trailing-edge flap for wind turbines can effectively improve the lift coefficient

and the lift-to-drag ratio. A movable trailing-edge flap provides a significant advantage for improving the load distribution of the whole blade, thereby reducing the power and mechanical load fluctuations caused by turbulent flow, wind shear, and tower shadow.

In this paper, an investigation of the effect of the trailing-edge flap on airfoil S809 was presented. The airfoil S809 is a laminar-flow airfoil with 21 % thickness and was specially designed for horizontal-axis wind turbine application [4][5]. Several wind tunnel tests were conducted for this airfoil at Colorado State University, Ohio State University and Delft University of Technology. Therfore, the airfoil S809 is selected as the basic airfoil of the trailing-edge flap which is a combination of the traditional flap and a special-shaped gurney flap (GF).The proposed trailing-edge flap model considers the gap structure between the flaps and the airfoil body. The aerodynamic performance and the flowfield of the proposed trailing edge flap airfoil are predicted by computational fluid dynamics (CFD) at angles of attack from -5° to 12.5°. The lift coefficient, drag coefficient, pressure contour, and streamline distribution of the proposed trailing-edge flap airfoil are analyzed and compared with traditional flaps.

2. Proposed trailing-edge flap model

2.1 The airfoil model with the proposed trailing-edge flap

The S809 airfoil is selected as the basic airfoil. The length of the airfoil chord b is 1000 mm. The length of the flap considerably influences the aerodynamic performance of the airfoil. Barlas [6] analyzed the changes in inflow and predicted the theoretically required flap angles and actuation frequencies for full control of all fluctuations in aerodynamic loads. The results indicate that 10% chord length trailing-edge flaps located near the tips can alleviate all aerodynamic load fluctuations with a range in flap deflections between +12° and +12° in normal power production cases. Therefore, the current study sets the flap length to 10% chord length. The gap ε between the flap and the airfoil body is set to 1 mm. The high of the proposed gurney flap is set to 1% chord length. In order to reduce the drag force, the proposed trailing-edge flap is adopts Triangle gurney flap with the vortex angle of 60°. And the triangle gurney flap is easier to install on the blades, such as sticking to the existing traditional flap.

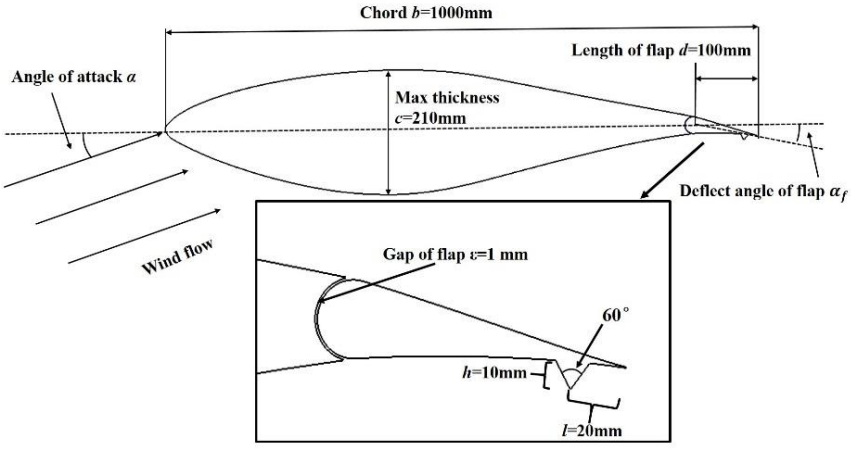

Fig. 1 Modeling of the S809 airfoil with the proposed trailing-edge flap

Ref. [7] on the influence of gurney flaps on the aerodynamic characteristics of the airfoil demonstrates that as the gurney flaps move forward from the trailing edge, the increase in lift coefficient decreases correspondingly and exerts a negative effect. Thus, a rising area is observed near the lower

surface of the trailing edge. Simulation and analysis indicate that the change in lift coefficient is not apparent when the gurney flap is near the trailing edge. With the small thickness of the trailing edge and poor bearing capacity considered, the gurney flap is installed on the flap from the 20 mm tip of the trailing-edge flap. The airfoil model with the proposed trailing-edge flap is shown in Fig. 1.

2.2 Computational grid

The grid adopts a 2-dimensional structured grid and a C grid topology. The distance from the leading edge of the airfoil to the inlet boundary of the flowfield is 20 times that of the chord. The distance from the trailing edge of the airfoil to the outlet boundary of the flowfield is also 20 times that of the chord. A total of 736 nodes surround the airfoil surface, and the first layer of the grid height is y=0.02 mm; y^+=0.85 is within a reasonable range. Meanwhile, 140 nodes can be observed from the inlet to the airfoil surface, and the total grid number is 178000. To verify grid independence, the flowfield model of grid numbers 120000, 150000, 178000, 200000 is calculated. The result shows that the convergence is good and the aerodynamic performance reaches a stable value when the grid number is greater than 150000.Therefore, a model with a grid number of 178,000 should be selected. The grid is shown in Fig. 3.

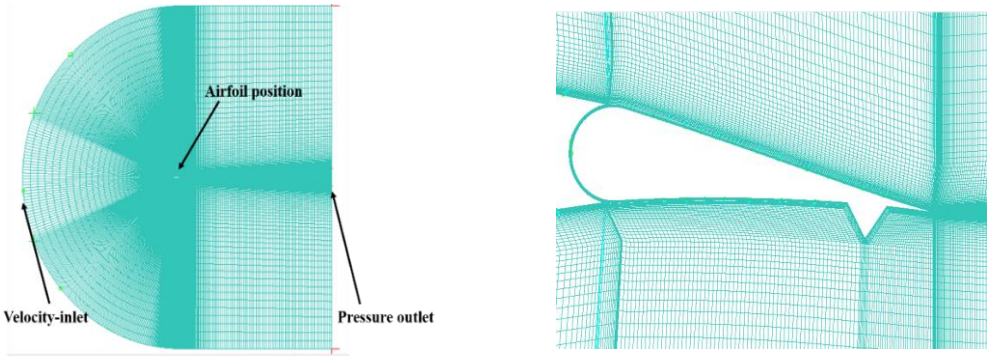

a. Grid structure of whole flowfield b. Grid structure of the trailing edge flap

Fig. 2 Grid structure of the flowfield around the airfoil

3. Calculation method and model validation

Owing to the low wind speed of the wind turbine, the flowfield near the blade can be considered as an incompressible viscous fluid. The solution is based on the incompressible Reynolds averaged Navier–Stokes (RANS) equations, which can be written as

$$\frac{\partial U_i}{\partial t}+\frac{\partial\left(U_iU_j\right)}{\partial x_j}=-\frac{1}{\rho_0}\frac{\partial P}{\partial x_i}+\nu\frac{\partial^2U_i}{\partial x_j^2}+f_i \tag{1}$$

$$\frac{\partial U_i}{\partial x_i}=0 \tag{2}$$

where U_i is velocity; P is incompressible pressure, ρ is density, v is kinematic viscosity, and f_i is the added body forces.

The most widely used commercial computational fluid dynamics (CFD) software ANSYS FLUENT 15.0 was selected as the N-S solver. The SST k-ω 2-equation turbulence model is selected in

simulating wind turbine blades. Eddy viscosity coefficient of the turbulence model, equation of k, and ω are as follows:

$$\mu_T = \gamma^* \frac{\rho k}{\omega} \tag{3}$$

$$\frac{\partial}{\partial t}(\rho k) + \frac{\partial}{\partial x_j}(\rho u_j k) = \tau_{ij}\frac{\partial u_i}{\partial x_j} - \beta^* \rho \omega k + \frac{\partial}{\partial x_i}\left[(\mu + \sigma^* \mu_T)\frac{\partial k}{\partial x_j}\right] \tag{4}$$

$$\frac{\partial}{\partial t}(\rho \omega) + \frac{\partial}{\partial x_j}(\rho u_j \omega) = (\gamma \omega / k)\tau_{ij}\frac{\partial u_i}{\partial x_j} - \beta \rho \omega^2 + \frac{\partial}{\partial x_j}\left[(\mu + \sigma \mu_T)\frac{\partial \omega}{\partial x_j}\right] \tag{5}$$

where t is time, x_i position vector, u_i velocity vector, ρ density, p pressure, μ molecular viscosity, τ_{ij} is the Reynolds stress tensor. k is the turbulent mixing energy and ω is the specific dissipation rate. The Reynolds number is set to 10^6. The expression and values of those variables are provided in Ref.[8][9].

The aerodynamic performance of the clean S809 airfoil model in the range of attack angle from 6.2° to 22.1° is calculated by using the RANS method. Fig. 3 shows that the CFD results are relatively close to the wind tunnel data within a wide range. Only when the angle of attack is greater than 17° the CFD results markedly deviate from the wind tunnel data; meanwhile the lift coefficient is slightly larger than the wind tunnel data, and the drag coefficient is smaller than the wind tunnel data. The reason is that the ideal boundary condition is assumed in CFD, and stall delay occurs near the stall angle.

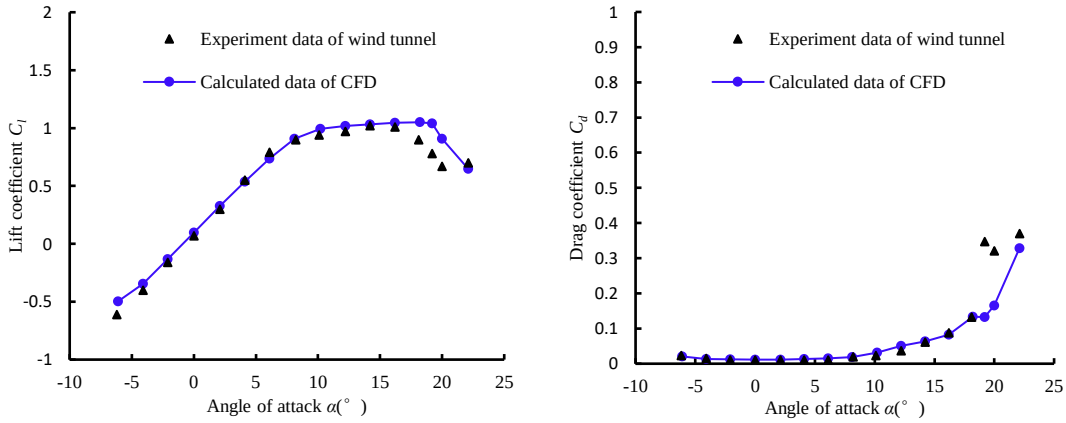

a. Lift coefficients vs. angle of attack b. Drag coefficients vs. angle of attack

Fig. 3 Lift and drag coefficients of the S809 airfoil

Wind turbine blades are generally controlled by the variable pitch controller, and the angle of attack near the tip is in the non-stall range. Thus, the angle of attack ranging from -5° to 12.5° in the study satisfies the research requirement.

4. Results and discussion

4.1 Effects of the gap

The proposed trailing-edge flap is rotatable, so the flap gap is inevitable. Although the gap can be filled with elastic materials, the analysis of the gap is also necessary. Theoretically, the gap between the

proposed trailing-edge flap and the airfoil body connects the upper surface and the lower surface flowfield, which can increase the upper surface pressure and reduce the lower surface pressure. Consequently, the gap decreases the lift coefficient of the airfoil, while negatively affecting the stall performance of the flaps. However, the gap is considerably small, and the effect on the aerodynamic performance of the airfoil has yet to be verified.

The pressure coefficient distributions of the proposed trailing-edge flaps with different sizes of the gaps and the model without gap are compared in the study. Fig. 4 shows the influence of different size of flap gaps on the pressure coefficient of the airfoil surface at 5° attack angle. It can be seen from the figure that the pressure coefficient is different after the gap is greater than 1 mm and the influence of the gap is mainly on the middle and posterior segment of the airfoil surface. The increase of upper surface pressure will obviously reduce the lift coefficient and have a negative effect on the stall performance of the airfoil. Therefore, we should limit the size of the proposed trailing-edge flap gap in applications.

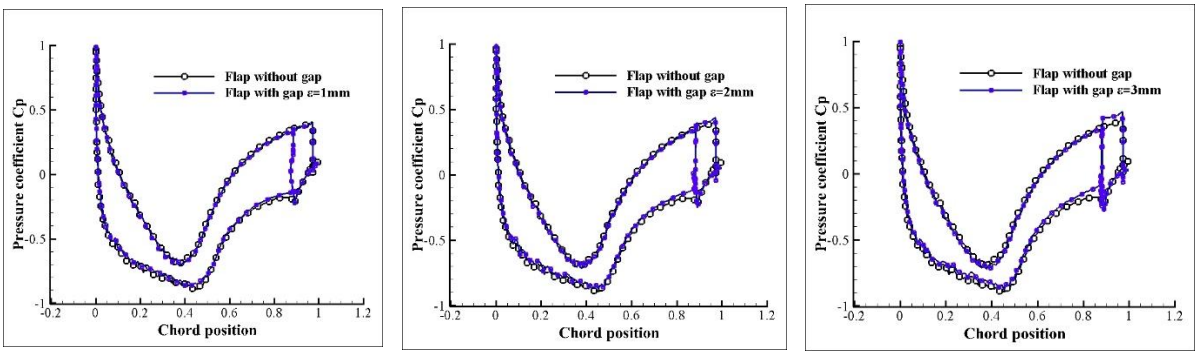

a. ε = 1 mm b. ε = 2 mm c. ε = 3 mm

Fig. 4 Pressure coefficient distributions of the airfoil with the proposed flaps with different gap size

4.2 Effects of flap deflection angle

The control performance of the proposed trailing-edge flap can be obtained by analyzing the aerodynamic characteristics of different flap deflection angles. Wind turbine blades are generally controlled by the variable pitch controller, and the angle of attack near the tip is in the non-stall range. The angles of attack 0°, 2.5° and 5° of the S809 airfoil were chosen. The flap deflection angle was changed from -5° to 10° at each angle of attack. Fig. 5 shows the effects of the divergent trailing edge and angle of attack on the aerodynamic characteristics of the airfoil. As shown in the figure, the proposed trailing-edge flap can effectively improve the lift coefficient of the airfoil under the same angle of attack, compared with the traditional flap. When the angle of attack is small, the lift-to-drag ratio increases; however, when the angle of attack is greater than 5°, the lift-to-drag coefficient decreases in the large flap deflection angles. Fig. 6 shows the pressure coefficient distributions of the airfoil with proposed flaps with different flap deflection angle at 0° attack angle. It can be seen that the airfoil with proposed flap has a larger pressure difference between the upper and lower surface, especially in the middle of the airfoil.

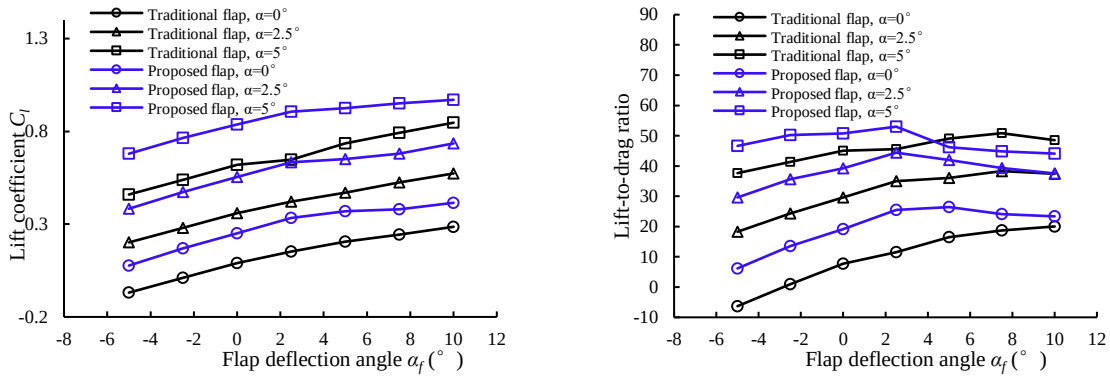

a. Lift coefficient vs. flap deflection angle b. Lift-to-drag ratio vs. flap deflection angle

Fig. 5 Effects of the divergent trailing edge and angle of attack on the aerodynamic characteristics of the airfoil

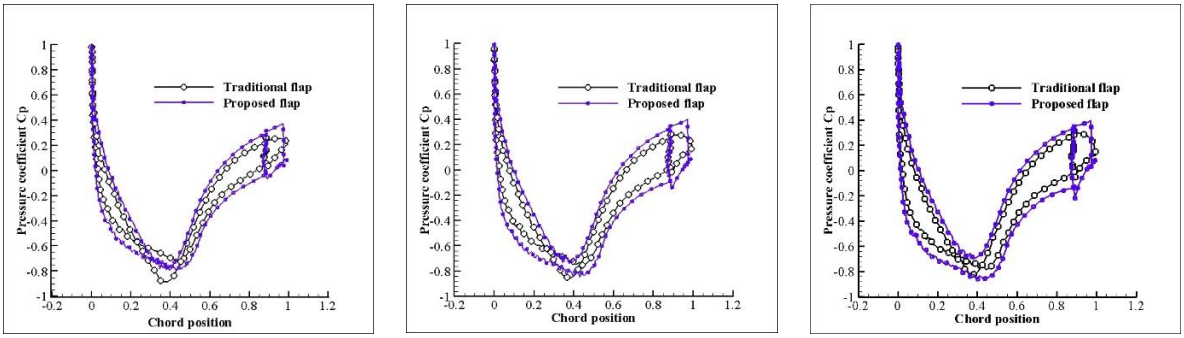

a. α_f=0° b. α_f=2.5° c. α_f=5°

Fig. 6 Pressure coefficient distributions of the airfoil with proposed flaps with different flap deflection angle

4.3 Effects of flap on the flowfield

The proposed trailing-edge flap combines traditional variable flaps and triangle gurney flaps. The effect of improving the lift coefficient is equal to an increase in the camber trailing edge of the airfoil. Figs. 7 and 7 are the flowfield distribution at the 5° angle of attack for the traditional flap and the proposed trailing-edge flap, respectively. As indicated in the comparison of pressure between the traditional flap and the proposed trailing-edge flap, the latter can markedly increase the pressure on the lower surface and reduce the pressure on the upper surface to improve the lift coefficient. The streamline distribution shows that with an increase in the angle of the flap, the vortex is generated; the larger the flap deflection angle, the stronger the vortex. Figs. 7 and 8 show that the proposed trailing-edge flaps can effectively reduce the vortex and the separation of the boundary layer at the trailing edge.

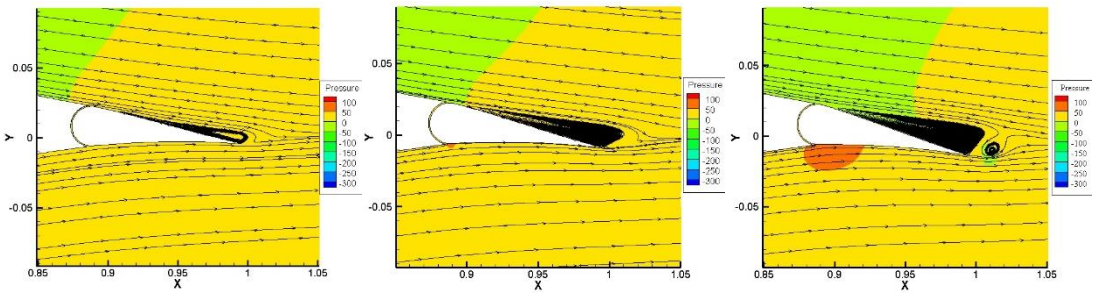

a. α_f=2.5° b. α_f=5° c. α_f=7.5°

Fig. 7. Streamline and pressure distribution of the airfoil with the traditional flap

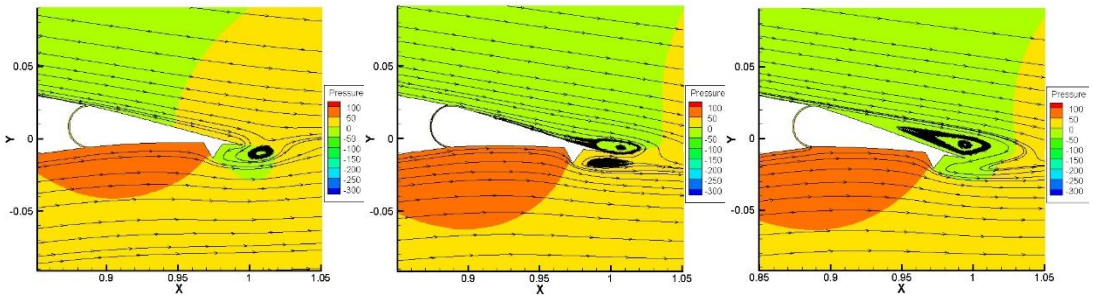

a. α_f=2.5° b. α_f=5° c. α_f=7.5°

Fig. 8. Streamline and pressure distribution of the airfoil with the proposed trailing-edge flap

5. Conclusion

In the study, a proposed trailing-edge flap is designed by adding a triangle gurney flap to the traditional variable trailing-edge flap. The aerodynamic performance and flowfield of the proposed trailing-edge flap airfoil are predicted. The results indicate that the gap between the flap and the airfoil body have a negative effect on the aerodynamic performance of the flaps when the size of the gap is greater than 1 mm. The proposed trailing-edge flap can significantly improve the lift coefficient and the lift-to-drag ratio of the airfoil, compared with the traditional flap. The better aerodynamic performance can be obtained at the small angle of attack. This characteristic can be used in designing the airfoil thickness at the flap. Finally, the streamlines of the traditional flaps and the proposed trailing-edge flaps are compared. The proposed trailing-edge flaps can effectively reduce the vortex and the separation of the boundary layer at the trailing edge.

However, more experimental studies on the performance of the 3D model need to be conducted in order to improve the control performance data of the proposed trailing-edge flaps.

Acknowledgments

This work was supported by Research Program of State Grid Corporation of China (Wind Turbine Aerodynamic-Mechanical-Electrical United Simulation and Assessment of Operation Characteristics).

References

[1] T. K. Barlas, G. A. M. van Kuik. Review of state of the art in smart rotor control research for wind turbines. Progress in Aerospace Sciences, 2010(46): 1-27.

[2] H. A. Madsen. Development of Smart Blade Technology-Trailing Edge Flaps. Roskilde, Danmark: DTU Wind Energy Annual Report, 2013: 12-13.

[3] L. Bergami, V. Riziotis, M, Gaunaa. Aerodynamic response of an airfoil section undergoing pitch motion and trailing edge flap deflection: a comparison of simulation methods. Wind Energy, 2014, 17(3): 389-406.

[4] Lee SG, Park SJ, Lee KS, Chung C. Performance prediction of NREL Phase VI blade adopting blunt trailing edge airfoil. Energy, 2012, 47(1): 47-61.

[5] Liu ZY, Wang XD, Kang S. Stochastic performance evaluation of horizontal axis wind turbine blades using non-deterministic CFD simulations. Energy, 2014. 73: 126-136.

[6] Barlas T, Lackner M. Smart rotor blade technology applied to the Upwind reference turbine. Proceedings of the IEA topical expert meeting on the application of smart structures for large wind turbine rotor blades, Sandia National Labs, Alberquerque, USA May 2008.

[7] Hao Lishu, Qiao Zhide, Song Weiping, Zhou Hong. Wind-tunnel investigation of aerodynamic force for airfoil using Gurney flap. Flight Dynamics, 2011, 29(04): 53-55.

[8] Alibek Issakhov. Modeling of Synthetic Turbulence Generation in Boundary Layer by Using Zonal RANS/LES Method. International Journal of Nonlinear Sciences and Numerical Simulation, 2014, 15(2).

[9] MENTER F R. Zonal two equation k-ω turbulence models for aerodynamic flows. AIAA-93-2906, 1993.